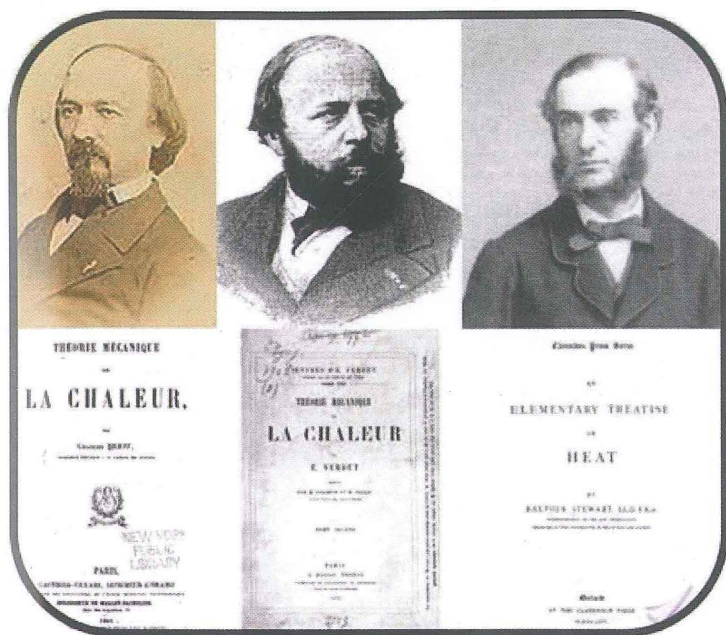


LA INVESTIGACIÓN DEL GRUPO ESPECIALIZADO DE TERMODINÁMICA DE LAS REALES SOCIEDADES ESPAÑOLAS DE FÍSICA Y DE QUÍMICA 2015



EDITORES:
MARTA MARÍA MATO CORZÓN
MANUEL MARTÍNEZ PIÑEIRO
JOSÉ LUIS LEGIDO SOTO

Universidade de Vigo



**La investigación del Grupo
Especializado de Termodinámica
de las Reales Sociedades Españolas
de Física y de Química.**

Vol. 7, año 2015

Editores:
Marta María Mato Corzón
Manuel Martínez Piñeiro
José Luis Legido Soto

ISBN: 978-84-8158-677-0

Imprime: Tórculo Comunicación Gráfica, S. A.
Edición 2015

Este volumen contiene una selección de las comunicaciones presentadas en la Reunión Termo 2014: XIV Encuentro Inter-Bienal del Grupo Especializado de Termodinámica (GET) de las Reales Sociedades Españolas de Física y Química celebrado del 14 al 16 Septiembre 2014 en el Talaso Atlántico de Baiona, Vigo.

COMITÉ CIENTÍFICO GET2014

Prof. M^a Inmaculada Paz Andrade, Universidade de Santiago de Compostela.

Prof. José Ramón Solana Quirós, Universidad de Cantabria.

Prof. Carlos Casanova Roque, Universidad de Valladolid.

Prof. Luís Romani Martínez, Universidade de Vigo.

Prof. Josefa Fernández Pérez, Universidade de Santiago de Compostela.

Prof. Óscar Cabeza Gras, Universidade de A Coruña.

Prof. Manuel Martínez Piñeiro, Universidade de Vigo.

COMITÉ ORGANIZADOR GET2014

Presidente: Prof. José Luis Legido Soto

Secretario: Prof. Manuel Martínez Piñeiro

Vocales:

Prof. Javier Vijande López
Prof. Marta María Mato Corzón
Prof. Luís Lugo Latas

Colaboradores:

Dra. Carmen Paula Gómez Pérez
Dña María Mercedes Riádigos García
D. Nicolás Legido García-Garabal

PRESENTACIÓNXI

ÍNDICE DE CAPÍTULOS

CAPÍTULO 1. SIMULACION MOLECULAR DE HIDRATOS DE CO₂.

J. M. Míguez, M. M. Conde, J. P. Torr , F. J. Blas, M. M. Pi eiro 1

CAPÍTULO 2. ANALISIS HIST RICO SOBRE EL ORIGEN DEL LLAMADO PRINCIPIO CERO DE LA TERMODINAMICA.

J. L. G mez Est vez 13

CAPÍTULO 3. ESTABILIDAD T RMICA Y EVALUACI N DE LA ENERG A DE ACTIVACI N DE L QUIDOS I NICOS.

J. J. Paraj , M. Villanueva, P. B. S nchez, J. Garc a, J. Salgado 23

CAPÍTULO 4. PERMITIVIDAD Y CONDUCTIVIDAD EL CTRICA DE NANOFLUIDOS DE  XIDO DE COBRE DE 12 NM EN BASE ETILENGLICOL A DIFERENTES TEMPERATURAS.

M. F. Coelho, M. A. Rivas, T. P. Iglesias 35

CAPÍTULO 5. CALIBRADO DE LOS CANALES T RMICOS DEL SAT LITE LANDSAT-8.

D. Caselles, V. Caselles, R. P rez, E. Valor, C. Do a, V. Garc a-Santos, R. Nicl s, M. J. Barber , J. S nchez, C. Coll 41

CAPÍTULO 6. MICROEMULSIONS WITH NONIONIC SURFACTANTS AND POTENTIAL DETERMINING IONS.

J. A. Manzanares, J. Cervera, S. Mafe, C. Johans 53

CAPÍTULO 7. AN LISIS DE LA VIABILIDAD DEL AUTOABASTECIMIENTO ENERG TICO DE UN MATADERO DE CERDO IB RICO CON ENERG AS RENOVABLES.

F. Cuadros Bl zquez, A. Gonz lez Gonz lez, F. Cuadros Salcedo 69

CAPÍTULO 8. FITORREMEDIACIÓN EN AGUAS DULCES CONTAMINADAS. <i>S. Gómez-Fernández, J. García, J. M. Torres, E. González-Romero</i>	79
CAPÍTULO 9. INVESTIGACIÓN SOBRE EL COMPORTAMIENTO TERMOFÍSICO DE MEZCLAS DE ARCILLAS CON DIFERENTES AGUAS PARA USO EN REHABILITACIÓN. <i>C. P. Gómez, R. Moscoso, L. Mourelle, L. M. Casás, J. L. Legido</i>	95
CAPÍTULO 10. DETERMINACIÓN DE CONDUCTIVIDAD TÉRMICA Y PROPIEDADES VISCOELÁSTICAS DE NANOFLUIDOS DERIVADOS DEL GRAFENO. <i>C. H. Merino, J. Calvo-Bravo, M. Pérez-Rodríguez, M. M. Piñeiro, M.J. Pastoriza-Gallego</i>	109
CAPÍTULO 11. CAPACIDADES CALORÍFICAS DE NANOPOLVOS DE ZNO, MGO Y ZRO ₂ Y NANOFLUIDOS BASADOS EN ETILENGLICOL A TEMPERATURAS DESDE 243.15 K HASTA 473.15 K. <i>D. Cabaleiro, J.L. Legido, L. Lugo</i>	121
CAPÍTULO 12. ESTUDIO DE LA SENSIBILIDAD DE LAS BACTERIAS A LA INFLUENCIA DE LOS ULTRASONIDOS UTILIZANDO TÉCNICAS MICROCALORIMÉTRICAS. <i>C. Vázquez, T. P. Iglesias, N. Lago, M. M. Mato, J. L. Legido</i>	133
CAPÍTULO 13. ESTUDIO EXPERIMENTAL DE LA MICROESTRUCTURA EN LA TRANSICIÓN LÍQUIDO-GEL DE LAS MEZCLAS DE EMIM-OS + AGUA. <i>O. Cabeza, E. Rilo, M. Domínguez-Pérez, L. Segade, S. García-Garabal, E. López-Lago, L. M. Varela Cabo</i>	143
CAPÍTULO 14. CAPACIDAD CALORÍFICA MOLAR DE MEZCLAS (1,8-CINEOL + ETANOL). MEDIDA Y MODELIZACIÓN MEDIANTE UNIFAC Y COSMO-RS. <i>J. F. Martínez, S. Schneider, J. I. Pardo, A. M. Mainar, J. S. Urieta</i>	157

CAPÍTULO 15. FABRICACIÓN Y EVALUACIÓN DE PROPIEDADES ELÉCTRICAS Y MECÁNICAS DE NANOCOMPUESTOS CONSTITUIDOS POR NANOLÁMINAS DE GRAFENO Y POLIPROPILENO.

M. J. Pastoriza-Gallego, M.M. Piñeiro, J. L. Legido, J. A. Covas..... 167

CAPÍTULO 16. MODELIZACIÓN DEL COMPORTAMIENTO PVT Y VISCOSIDAD PARA LÍQUIDOS IÓNICOS.

P. B. Sánchez, M. M. Mato, J. L. Legido, J. García..... 177

CAPÍTULO 17. ESTUDIO DFT DE LOS POTENCIALES DE INTERACCIÓN DE CO₂ Y CH₄ EN EL INTERIOR DEL HIDRATO TIPO I.

M. Pérez-Rodríguez, A. Vidal-Vidal, M. M. Piñeiro 187

CAPÍTULO 18. ESTUDIO DE LA DENSIDAD A PRESIÓN DE SISTEMAS BINARIOS Y TERNARIOS DIALQUILCARBONATO + N-ALCANO + P-XILENO.

A. M. Gayol, L. M. Casás, J. L. Legido..... 197

CAPÍTULO 19. TOXICIDAD DE LÍQUIDOS IÓNICOS DERIVADOS DEL IMIDAZOLIO: EFECTOS SOBRE LA ACTIVIDAD MICROBIANA DEL SUELO Y LA GERMINACIÓN DE SEMILLAS.

J. Salgado, J.J. Parajó, P. V. Verdes, M.Villanueva, J.A. Rodríguez-Añón, J. Proupín, O. Reyes..... 209

CAPÍTULO 20. CÁLCULO TEÓRICO DE LOS TRES PRIMEROS TÉRMINOS PERTURBATIVOS DE LA ENERGÍA LIBRE DE UN FLUIDO DE LENNARD-JONES CON NÚCLEO DURO.

J. Largo, J. R. Solana..... 221

CAPÍTULO 21. TENSIÓN SUPERFICIAL DE N-ALCOHOLES Y ALCOHOLES ALIFÁTICOS. SELECCIÓN DE DATOS Y CORRELACIÓN CON LA TEMPERATURA.

I. Cachadiña, A. Mulero, E. L. Sanjuán, M. I Parra 231

MICROEMULSIONS WITH NONIONIC SURFACTANTS AND POTENTIAL DETERMINING IONS

José A. Manzanares,^{a,b} Javier Cervera,^a Salvador Mafé,^a Christoffer Johans^b

^a *Departament de F.T. y Termodinàmica, Universitat de València, 46100 Burjassot*

^b *Department of Chemistry, Aalto University, FI-0076 Aalto, Finland*

E-mail: manzanar@uv.es

Abstract

When added to immiscible liquid-liquid systems, the ions with different hydrophobicity forming a potential determining salt (PDS) reach a distribution equilibrium and generate an electrical potential difference. In microemulsions, the interfacial area per volume is so large that the total amount of charge that would be required to establish the macroscopic distribution potential exceeds the total charge present in the system. Consequently, the distribution potential is smaller than its macroscopic value and large deviations from local electroneutrality are observed. In this work the electrical polarization of a lamellar and w/o microemulsions composed of the aqueous solution of a PDS, an oil and a non-ionic surfactant is studied in order to explain the dependence of the distribution potential on the nature and concentration of the PDS, the surfactant concentration, and the geometry of the emulsion microstructure.

Keywords: Distribution potential, Microemulsions, Liquid-liquid interfaces

INTRODUCTION

Microemulsions are thermodynamically stable and macroscopically isotropic mixtures of two immiscible solvents and, at least, one amphiphilic component [1]. Their applications are mostly based on their extraordinary solubilisation capacity and the very high interfacial area per volume. The spatial confinement of chemical reactions in colloidal solutions and microemulsions enables, e.g., the size control in the synthesis of metal nanoparticles [2-4].

In liquid-liquid electrochemistry electrical potential differences can be applied without electrodes [5]. Electrified microemulsions are charged microheterogeneous systems with variable interfacial potential differences which is also controlled by the partitioning of ions [6-10]. This interfacial potential difference modifies, e.g., the interfacial tension as is known in electrocapillarity [11,12]. Potential determining salts (PDS) are strong electrolytes formed by ions of different hydrophobicity. When added to immiscible liquid-liquid systems, the dissociated ions redistribute in the aqueous and organic phases and generate the so-called distribution potential [13-17]. In a macroscopic system, the distribution potential $\Delta^{\infty}\phi_s$ can be established on account of the unlimited amount of available ions (and charge). In microemulsions, the interfacial area per volume is so large that the charge required to establish the distribution potential $\Delta^{\infty}\phi_s$ across every microinterface can easily exceed the charge of all the ions present in the system. As a consequence, the distribution potential in microemulsions is

smaller than in macroscopic systems $\Delta_o^w\phi \leq \Delta_o^w\phi_x$ and depends on the salt concentration.

The standard description of the distribution potential in liquid-liquid electrochemistry makes use of the electroneutrality condition far from the interface because the aqueous and organic phases are thought of as a spatially charged region close to the interface and a locally electroneutral region further away [13]. However, the electrical double layer may cover the entire extension of both phases in electrified microemulsions. For example, when a PDS like tetradecylammonium chloride is added to the microemulsion, the ions partition into different phases so that, for the range of salt concentrations of practical interest, the aqueous phase only contains hydrophilic chloride anions and the organic phase only contains hydrophobic cations [8]. The importance of the problem of significant deviations from local electroneutrality in small systems like electrified microemulsions has frequently been recognized but its solution has only been derived in the case of small potentials and for nanodroplets in a continuum phase [14,17-20].

Electrified microemulsions with PDS have several distinctive features that make them different from macroscopic immiscible electrolyte solutions (ITIES) and from ordinary microemulsions, either with ionic or non-ionic surfactants. The dissociated ions accumulate at both sides of the interface and stabilize the microemulsion, which may be formed even in the absence of surfactant [21]. The distribution potential $\Delta_o^w\phi$ in electrified microemulsions can be varied from 0 to that of macroscopic ITIES, $\Delta_o^w\phi_x$. Since the charge transfer kinetics in microheterogeneous media is affected by the interfacial potential, this simple and convenient procedure for potential variation can be exploited to affect the rate of processes such as proton transfer reactions [10].

For surfactant volume fractions higher than that of the \tilde{X} point of the microemulsion where the three-phase body meets the one phase region (i.e., in the tail of Kahlweit's fish phase diagram) [1,8], an increase in temperature produces a phase change from o/w microemulsion (oil swollen micelles in aqueous continuous phase) to lamellar structure, and then to w/o microemulsion (water-in-oil or swollen reverse micelles). In the next section, the electrical polarization of lamellar and w/o microemulsions composed of the aqueous solution of a PDS, an oil and a non-ionic surfactant is described in order to explain the dependence of the distribution potential on the nature and concentration of the PDS and the surfactant concentration. The theoretical modelling incorporates naturally the effect of the phase volume ratio [22] and does not use local electroneutrality. Global electroneutrality is imposed using the cell model [23]. The evaluation of the distribution potential requires matching the solutions of the Poisson-Boltzmann equation (PBE) in the different phases. The PBE is solved analytically in lamellar electrified microemulsions. Approximate solutions for lamellar and micellar microemulsions are also derived and compared to exact numerical results.

THEORETICAL MODELLING

Microemulsion composition and cell dimensions. The aqueous solution of a PDS, a non-ionic surfactant, and an organic solvent that (initially) contains no salt are considered as three (pseudo)components of the microemulsion. Their concentrations are specified by their volume fractions Φ_w , Φ_s and $\Phi_o = 1 - \Phi_w - \Phi_s$, respectively. It is assumed that the surfactant is in micellar w/o or lamellar form, with no monomers in solution and that the surfactant monolayer contains no ions, water and oil molecules. The microemulsion volume is divided into globally electroneutral cells, and only one such cell consisting of aqueous (w), surfactant (s), and oil (o) regions is considered henceforth. The cell extends from $r = 0$ to $r = L$, where r is the coordinate normal to the surfactant monolayer; this coordinate is axial or radial depending on the microemulsion geometry. The aqueous phase extends from $r = 0$ to $r = L_w$, the surfactant monolayer from $r = L_w$ to $r = L_w + L_s$, where L_s is the surfactant length (headgroup plus tail), and the organic phase extends from $r = L - L_o$ to $r = L = L_w + L_s + L_o$. The cell volume is $V = 4\pi L^3/3$ in the micellar case and $V = AL$ in the lamellar case, where A is the lamellar area.

Since the components are immiscible, the volume of phase j is $V_j = \Phi_j V$ ($j = w, s, o$). In lamellar microemulsions, a similar relation holds for the thicknesses $L_j = \Phi_j L$. In micellar microemulsions, $L_w = \Phi_w^{1/3} L$ and $L_o = L - L_w - L_s$ where the total cell size $L = L_s / [(1 - \Phi_o)^{1/3} - \Phi_w^{1/3}]$ is evaluated as a function of the effective length L_s of the surfactant molecule. Thus, L_w , L_o and L increase with decreasing Φ_s . When oil and water are in the same volume ratio, $\Phi_w = \Phi_o = (1 - \Phi_s)/2$, the aqueous and organic regions have the same thickness in the lamellar case, but different thicknesses in the micellar case, with the external organic region being thinner. In lamellar microemulsions, the areas of the water-surfactant and oil-surfactant interfaces are $A_w = A_o = A$, and therefore $A_w L_w / V_w = A_o L_o / V_o = 1$. In w/o micelles, these areas are $A_w = 4\pi L_w^2$ and $A_o = 4\pi(L - L_o)^2$, and therefore $A_w L_w / V_w = 3$ and $A_o L_o / V_o = 3[(1 - \Phi_o)^{2/3} - (1 - \Phi_o)] / \Phi_o = 3(L - L_o)^2 / (3L^2 - 3LL_o + L_o^2)$. For the case $\Phi_w = \Phi_o$, the latter ratio ranges from 0.780 when $\Phi_s \rightarrow 0$ to 1 when $\Phi_s \rightarrow 1$.

Equilibrium ion distribution. Prior to the microemulsion formation, the aqueous solution has a molar concentration c of the 1:1 PDS. Once these ions reach an equilibrium distribution between the phases w and o so that the electrolyte mean molar concentrations $c_{\pm w} \equiv (c_{1w} c_{2w})^{1/2}$ and $c_{\pm o} \equiv (c_{1o} c_{2o})^{1/2}$ are independent of position (within the respective phase). The distribution potential is defined as the resulting potential difference between the ionic solutions at $r = 0$ and $r = L$, the furthest positions from the interface, $\Delta_w^\circ \phi \equiv \phi(0) - \phi(L)$. The electrolyte chemical partition coefficient is

$$K_{w/o} \equiv \exp[z_1 f (\Delta_o^w \phi_1^\circ - \Delta_o^w \phi_2^\circ) / 2] = c_{\pm w} / c_{\pm o} \quad (1)$$

where $f \equiv F/RT$, z_i is the charge number of species i ($z_1 = -z_2$), $\Delta_o^w \phi_i^\circ \equiv -\Delta G_{tr,i}^{\circ,o \rightarrow w} / z_i F$ is its standard transfer potential, and $\Delta G_{tr,i}^{\circ,o \rightarrow w}$ is its standard Gibbs free energy of transfer from phase o to w. Formal and standard transfer potentials are usually considered as equivalent when calculating the

distribution potential [22]. The equilibrium with respect to the ion distribution between these solutions requires

$$c_{iw}(0)\exp[z_i f(\Delta_o^w \phi - \Delta_o^w \phi_i^*)] = c_{io}(L), \quad i = 1, 2. \quad (2)$$

If the solutions at $r = 0$ and $r = L$ were electroneutral, then $c_{iw}(0) = c_{\pm w, \infty}$ and $c_{io}(L) = c_{\pm o, \infty}$ ($i = 1, 2$), and the distribution potential would take the macroscopic value $\Delta_o^w \phi_{\infty} = (\Delta_o^w \phi_1^* + \Delta_o^w \phi_2^*) / 2$, independently of the salt concentration c and the volume fractions of the microemulsion components [14-17]. When the two ions have similar hydrophobicity ($\Delta_o^w \phi_1^* \approx -\Delta_o^w \phi_2^*$) the distribution potential $\Delta_o^w \phi_{\infty}$ is small, but it can range between -0.7 and $+0.7$ V for some PDS. For salts composed of a hydrophilic cation ($\Delta_o^w \phi_1^* > 0$) and a hydrophobic anion ($\Delta_o^w \phi_2^* > 0$), the aqueous phase acquires an excess of positive charge (due to the higher affinity of the cation for this phase) and the organic phase acquires an excess of negative charge, so that the former is positive with respect to the latter, $\Delta_o^w \phi_{\infty} > 0$. Contrarily, $\Delta_o^w \phi_{\infty} < 0$ when the salt is composed of a hydrophobic cation ($\Delta_o^w \phi_1^* < 0$) and a hydrophilic anion ($\Delta_o^w \phi_2^* < 0$). We use label 1 for the more hydrophilic species, so that $z_1 \Delta_o^w \phi > 0$ and $\Delta G_{r,2}^{s,o \rightarrow w} > \Delta G_{r,1}^{s,o \rightarrow w}$.

Equation (2) implies that the (dimensionless) distribution potential is

$$z_1 f \Delta_o^w \phi = z_1 f \Delta_o^w \phi_{\infty} + (1/2) \ln(\alpha_o \alpha_w) = z_1 f \Delta_o^w \phi_{\infty} - \varphi_{o0} - \varphi_{ow}, \quad (3)$$

where the ratios $\alpha_w \equiv c_{2w}(0) / c_{1w}(0) \equiv e^{-2\varphi_{ow}} \leq 1$ and $\alpha_o \equiv c_{1o}(L) / c_{2o}(L) \equiv e^{-2\varphi_{o0}} \leq 1$ quantify the deviations from local electroneutrality at $r = 0$ and $r = L$. Equation (3) can be conveniently interpreted as follows (Fig. 1). The microemulsion is in distribution equilibrium with fictitious electroneutral aqueous and organic solutions whose electrolyte concentrations are $c_{\pm w}$ and $c_{\pm o}$, respectively. The dimensionless potential difference between these solutions is the macroscopic distribution potential and can be decomposed in three contributions, $z_1 f \Delta_o^w \phi_{\infty} = \varphi_{ow} + z_1 f \Delta_o^w \phi + \varphi_{o0}$, where $\varphi_{o0} = -(1/2) \ln \alpha_o \geq 0$ is the potential of the solution at $r = L$ with respect to the electroneutral organic solution, $z_1 f \Delta_o^w \phi \geq 0$ is the distribution potential in the microemulsion, and $\varphi_{ow} = -(1/2) \ln \alpha_w \geq 0$ is the potential of the electroneutral aqueous solution with respect to the solution at $r = 0$. In turn, the distribution potential is the sum of the potential drops in the phases o, s and w, $z_1 f \Delta_o^w \phi = \Delta \varphi_o + \Delta \varphi_s + \Delta \varphi_w$ (Fig. 1).

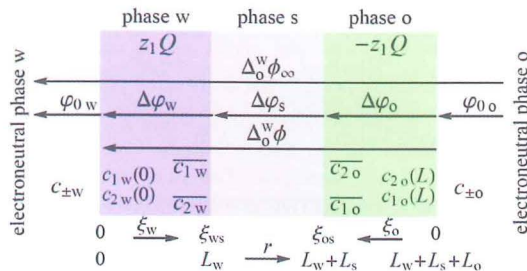


Figure 1. Schematic representation of the different potential drops in the electrified microemulsion regions, including the extensions of the phases and the ionic and electrolyte concentrations. The fictitious electroneutral phases in equilibrium with the microemulsion help to understand that the distribution potential in electrified microemulsions is smaller than in macroscopic ITIES.

Conservation equations. Due to the difference in hydrophobicity of the ions, phase w contains an excess of species 1, $\bar{c}_{1w} > \bar{c}_{2w}$, and phase o an excess of species 2, $\bar{c}_{2o} > \bar{c}_{1o}$. Then, these phases are not electroneutral but charged, and the total charge is $z_1 Q$ in phase w and $-z_1 Q$ in phase o. The majority ions (1 in phase w and 2 in phase o) are called counterions because they counterbalance most of the electric charge in the opposite phase. The concentrations of the minority ions, $c_w \equiv \bar{c}_{2w}$ and $c_o \equiv \bar{c}_{1o}$, are known as the stoichiometric electrolyte concentrations [24,25], and they differ significantly from the mean concentrations $c_{\pm w}$ and $c_{\pm o}$. The average concentrations in the phases w and o, \bar{c}_{1w} and \bar{c}_{1o} , respectively, satisfy the mass conservation equations

$$\Phi_w \bar{c}_{1w} + \Phi_o \bar{c}_{1o} = \Phi_w c \equiv c_T, \quad i = 1, 2, \quad (4)$$

where $c_T \equiv \Phi_w c$ is the total electrolyte concentration referred to the microemulsion volume. The average counterion concentrations $\bar{c}_{1w} = c - c_o / r_{w/o}$ and $\bar{c}_{2o} = (c - c_w) r_{w/o}$ can be expressed in terms of c_w and c_o and the volume fraction ratio $r_{w/o} \equiv \Phi_w / \Phi_o$. Similarly, the charge is expressed in terms of c_w and c_o as

$$Q / FV \equiv \Phi_w (\bar{c}_{1w} - \bar{c}_{2w}) = \Phi_o (\bar{c}_{2o} - \bar{c}_{1o}) = c_T - \Phi_w c_w - \Phi_o c_o \geq 0. \quad (5)$$

The evaluation of $\Delta_w^w \phi$ requires matching the solutions of the PBE in the three phases so that Eqs. (1) and (3) are satisfied; c_w and c_o can be found from these two conditions.

Poisson-Boltzmann equation (PBE). The Debye parameters are defined with respect to the total ionic concentration at $r = 0$ and $r = L$ as

$$\kappa_w^2 \equiv \frac{F^2 [c_{1w}(0) + c_{2w}(0)]}{\varepsilon_0 \varepsilon_w RT}, \quad \kappa_o^2 \equiv \frac{F^2 [c_{1o}(L) + c_{2o}(L)]}{\varepsilon_0 \varepsilon_o RT} \quad (6)$$

where ε_0 is the electrical permittivity of vacuum, and ε_w and ε_o are the relative permittivities of phases w and o. The average counterion concentrations are presented in dimensionless form as $\bar{c}_{kj}^2 \equiv F^2 \bar{c}_{kj} L_j^2 / \varepsilon_0 \varepsilon_j RT$, where $k = 1$ if $j = w$ and $k = 2$ if $j = o$.

The local ion concentrations in phase w are $c_{1w}(r) = c_{1w}(0)e^{\varphi_w}$ and $c_{2w}(r) = c_{1w}(0)\alpha_w e^{-\varphi_w}$ where $\varphi_w \equiv -z_1 f[\phi(r) - \phi(0)] \geq 0$ is the local dimensionless electric potential. The planar and spherical geometries are described simultaneously using a parameter m that takes the values 0 and 2, respectively. The PBE in this phase is

$$\frac{d^2 \varphi_w}{d\xi_w^2} + \frac{m}{\xi_w} \frac{d\varphi_w}{d\xi_w} = \frac{e^{\varphi_w} - \alpha_w e^{-\varphi_w}}{1 + \alpha_w} = \sinh \varphi_w + \tanh \varphi_{0w} \cosh \varphi_w \quad (7)$$

where $\xi_w = \kappa_w r$ is the dimensionless position. The r.h.s. of Eq. (7) reduces to e^{φ_w} when $\tanh \varphi_{0w} \approx 1$ (or $\alpha_w \approx 0$) and to $\sinh \varphi_w$ when $\varphi_{0w} \approx 0$ (or $\alpha_w \approx 1$) which are, respectively, the limits corresponding to absence of salt (i.e., only counterions present in phase w) and high salt concentration or macroscopic system (i.e., local electroneutrality at $r = 0$). The boundary conditions are $\varphi_w(0) = 0$, $(d\varphi_w / d\xi_w)_{\xi_w=0} = 0$ and

$$\left(\frac{d\varphi_w}{d\xi_{ws}}\right)_{\xi_{ws}} = \frac{2fQ}{\xi_{ws}C_{w0}} \quad (8)$$

where $\xi_{ws} \equiv \kappa_w L_w$ and $C_{w0} \equiv 2\varepsilon_0 \varepsilon_w A_w / L_w$. From known values of Q and \bar{c}_{1w} , the unknown parameters $\alpha_w \equiv e^{-2\varphi_{1w}}$ and ξ_{ws} can be determined using Eq. (8) and

$$\bar{\xi}_{1w}^2 \equiv \frac{F^2 \bar{c}_{1w} L_w^2}{\varepsilon_0 \varepsilon_w RT} = \frac{m+1}{\xi_{ws}^{m-1} (1+\alpha_w)} \int_0^{\xi_{ws}} e^{\varphi_w} \xi_w^m d\xi_w \quad (9)$$

The unknown concentrations $c_{1w}(0)$ and $c_{2w}(0)$ and the potential drop $\Delta\varphi_w \equiv \varphi_w(\xi_{ws}) \equiv z_1 f \Delta\phi_w \equiv z_1 f [\phi_w(0) - \phi_w(L_w)]$ can also be calculated from the solution of Eq. (7).

Similarly, the local ion concentrations in phase o are $c_{2o}(r) = c_{2o}(L)e^{\varphi_o}$ and $c_{1o}(r) = c_{2o}(L)\alpha_o e^{-\varphi_o}$ where $\varphi_o \equiv z_1 f [\phi(r) - \phi(L)] \geq 0$. The PBE in this phase is

$$\frac{d^2\varphi_o}{d\xi_o^2} - \frac{m}{\xi_{oL} - \xi_o} \frac{d\varphi_o}{d\xi_o} = \frac{e^{\varphi_o} - \alpha_o e^{-\varphi_o}}{1 + \alpha_o} = \sinh\varphi_o + \tanh\varphi_{o0} \cosh\varphi_o \quad (10)$$

where $\xi_o \equiv \kappa_o(L-r)$ is the dimensionless position and $\xi_{oL} \equiv \kappa_o L$; i. e., $\xi_{oL} - \xi_o = \kappa_o r$. Its boundary conditions are $\varphi_o(0) = 0$, $(d\varphi_o/d\xi_o)_{\xi_o=0} = 0$ and

$$\left(\frac{d\varphi_o}{d\xi_o}\right)_{\xi_{oL}} = \frac{2fQ}{\xi_{os}C_{o0}} \quad (11)$$

where $\xi_{os} \equiv \kappa_o L_o$ and $C_{o0} \equiv 2\varepsilon_0 \varepsilon_o A_o / L_o$. From Q and \bar{c}_{2o} , the unknown parameters $\alpha_o \equiv e^{-2\varphi_{o0}}$ and ξ_{os} can be determined using Eq. (11) and

$$\bar{\xi}_{2o}^2 \equiv \frac{F^2 \bar{c}_{2o} L_o^2}{\varepsilon_0 \varepsilon_o RT} = \frac{(m+1)\xi_{os}^2}{\xi_{oL} \xi_{os}^{m+1} (1+\alpha_o)} \int_0^{\xi_{os}} e^{\varphi_o} (\xi_{oL} - \xi_o)^m d\xi_o \quad (12)$$

Then, the unknown concentrations $c_{1o}(L)$ and $c_{2o}(L)$, and the potential drop in phase o $\Delta\varphi_o \equiv \varphi_o(\xi_{os}) \equiv z_1 f \Delta\phi_o \equiv z_1 f [\phi_o(L - L_o) - \phi_o(L)]$, can also be calculated.

In the surfactant monolayer with no ions, the continuity of the (normal component of the) electrical displacement requires

$$\Delta\varphi_s \equiv z_1 f \Delta\phi_s \equiv z_1 f [\phi(L_w) - \phi(L - L_o)] = fQ/C_s \quad (13)$$

where $C_s = \varepsilon_o \varepsilon_s (A_w A_o)^{1/2} / L_s$ is the electrical capacitance of the monolayer.

Differential capacitance. The differential capacitance of the cell is

$$\frac{1}{C} \equiv \frac{1}{z_1} \frac{d\Delta\varphi_o}{dQ} = \frac{1}{f} \left(\frac{d\Delta\varphi_w}{dQ} + \frac{d\Delta\varphi_s}{dQ} + \frac{d\Delta\varphi_o}{dQ} \right) \equiv \frac{1}{C_w} + \frac{1}{C_s} + \frac{1}{C_o} \quad (14)$$

when this monolayer has a low effective relative permittivity and the surfactant molecules are relatively long. The contribution from the phases s and o can be similar in magnitude, while the capacitance of phase w is usually much larger. The cell capacitance when $c_T \rightarrow 0$ is an important characteristic of the microemulsion which can be evaluated as follows. In this limit, the space charge density in the phases w and o is practically independent of position, and then the

r.h.s. of Eqs. (7) and (10) can be approximated by 1. Thus, it is obtained that $\Delta\phi_w \approx \xi_{ws}^2/2(m+1) \approx fQ/C_{w0}$, and hence the limit of C_w when $c_T \rightarrow 0$ is C_{w0} ; note that $m+1 = A_w L_w/V_w$. Similarly it is deduced that $\Delta\phi_o \approx \xi_{os}^2[(m+1)L-L_o]/[2(m+1)(L-L_o)]$. On the other hand, it is deduced that $2fQ/C_{o0} \approx \xi_{os}^2 V_o/A_o L_o$ where, as shown above, $A_o L_o/V_o = 1$ in the lamellar case and $A_o L_o/V_o = 3(L-L_o)^2/(3L^2-3LL_o+L_o^2)$ in the micellar case. We define the value of C_o in the limit $c_T \rightarrow 0$ as C'_{o0} . In the lamellar case $C'_{o0} = C_{o0}$, while the ratio $C'_{o0}/C_{o0} = (3L^2-3LL_o+L_o^2)/[(L-L_o)(3L-L_o)]$ ranges from 1 when $\Phi_o = 0$ to 1.093 when $\Phi_o = 1/2$ in the micellar case. Therefore, the cell capacitance in the limit $c_T \rightarrow 0$ is $C_0 = (C_{w0}^{-1} + C_s^{-1} + C_{o0}'^{-1}) \approx (C_{w0}^{-1} + C_s^{-1} + C_{o0}^{-1})$.

Polarization regimes. The charge separation required to build up the distribution potential depends on the characteristics of the microemulsion and, particularly, on its interfacial capacitance. The comparison between the charge available in the microemulsion and the charge required to establish the macroscopic distribution potential $\Delta_o^w \phi_x$ determines a critical value that separates two regimes where the electrical polarization of the microemulsion has different characteristics. The charge required to establish the distribution potential $\Delta_o^w \phi_x$ can be roughly estimated as $Q_{cr} \equiv C_o z_1 \Delta_o^w \phi_x$. For a given concentration c_T , the maximum charge separation that can be achieved is $Q_{max} \equiv FC_T V$. The two concentration regimes mentioned above correspond to $Q_{max} < Q_{cr}$ and $Q_{max} > Q_{cr}$. Alternatively, they can be described as $c < c_{cr}$ and $c > c_{cr}$ or $c_T < c_{T,cr}$ and $c_T > c_{T,cr} = \Phi_w c_{cr}$. It is important to observe that $c_{T,cr} \equiv C_o z_1 \Delta_o^w \phi_x / FV$ is proportional to the interfacial area per volume. The regime $c_T < c_{T,cr}$ cannot be observed in macroscopic ITIES because $c_{T,cr}$ is extremely small for those systems. The different behaviour of electrified microemulsions and macroscopic ITIES is more evident for large Φ_s , because $c_{T,cr}$ increases with increasing Φ_s .

Below the critical concentration, $c_T < c_{T,cr}$, the solvation energy contribution dominates and the minimization of the microemulsion free energy is achieved by maximizing the charge separation, $Q \approx Q_{max} \equiv FC_T V$. The phases w and o contain only counterions and the stoichiometric electrolyte concentrations c_w and c_o practically vanish, even though this implies a very low microemulsion entropy (viz., the contribution associated with the ion distribution). The distribution potential $z_1 \Delta_o^w \phi$ also increases linearly with c_T as $z_1 \Delta_o^w \phi \approx Q/C_o$. Since Q/c_T and $z_1 \Delta_o^w \phi/c_T$ take maximum values, we refer to this regime as that of maximum electrical polarization of the microemulsion. The regime is also characterized by the approximation $\tanh \phi_{o_j} \approx 1$ ($j = w, o$) because the ratios α_w and α_o take very small values (i.e., the deviations from local electroneutrality at $r = 0$ and $r = L$ are extreme), although they cannot vanish because the condition $z_1 f \Delta_o^w \phi \geq 0$ and Eq. (3) imply that $\alpha_w \alpha_o \geq \exp(-2z_1 f \Delta_o^w \phi_x)$. At low salt concentrations, $\phi_{ow} = -(1/2) \ln \alpha_w \approx [z_1 f (\Delta_o^w \phi_x^2 - \Delta_o^w \phi) - \ln r_{w/o}]/2$ and $\phi_{oo} = -(1/2) \ln \alpha_o \approx [z_1 f (\Delta_o^w \phi_x^2 - \Delta_o^w \phi) + \ln r_{w/o}]/2$ decrease linearly and $\Delta\phi_w \approx fFc_T V/C_{w0}$, $\Delta\phi_s \approx fFc_T V/C_s$ and $\Delta\phi_o \approx fFc_T V/C_{o0}$ increase linearly with increasing c_T .

For salt concentrations above the critical value, $c > c_{cr}$, the average ionic concentrations are $\bar{c}_{1w} \approx (c_{cr} + K_{w/o} r_{w/o} c)/(1 + K_{w/o} r_{w/o})$, $\bar{c}_{1o} \approx r_{w/o} (c - c_{cr})/(1 + K_{w/o} r_{w/o})$, $\bar{c}_{2w} \approx K_{w/o} \bar{c}_{1o}$, and $\bar{c}_{2o} \approx r_{w/o} (c + K_{w/o} r_{w/o} c_{cr})/(1 + K_{w/o} r_{w/o})$, so that $Q \equiv F(\bar{c}_{1w} - \bar{c}_{2w})V_w \approx Q_{cr} \equiv Fc_{cr} V_w$.

Upon increasing the salt concentration, the solutions at $r = 0$ and $r = L$ asymptotically approach local electroneutrality, i.e. α_w and α_o tend to 1, while $z_1\Delta_o^w\phi$ saturates to its maximum value $z_1\Delta_o^w\phi_o$. The potential drops in the phases w and o decrease slowly with increasing c_T but they cannot vanish.

Solution of the linearized PBE in lamellar and micellar microemulsions. For surfactants with low relative permittivity ϵ_s and relatively large thickness L_s , the potential drop $\Delta\phi_s$ across the surfactant monolayer is the larger contribution to the distribution potential $\Delta_o^w\phi \approx \phi(0) - \phi(L)$. Because of its larger relative permittivity, the potential drop in phase w is smaller (in magnitude) than in phase o, and they both are smaller than $\Delta\phi_s$. Thus, the r.h.s. of Eq. (7) can then be linearized to $\varphi_w + \tanh\varphi_{0w}$. Similarly, the r.h.s. of Eq. (10) can be linearized to $\varphi_o + \tanh\varphi_{0o}$ when the potential drop in phase o is small. In the lamellar case ($m = 0$), the potential is then approximately given by

$$\varphi_j(\xi_j) = \tanh\varphi_{0j}(\cosh\xi_j - 1) \quad (j = w, o) \quad (15)$$

so that Eqs. (8) and (11) reduce to

$$2fQ/C_{j0} = \tanh\varphi_{0j}(\xi_{js} \sinh\xi_{js}) \quad (j = w, o) \quad (16)$$

and Eqs. (9) and (12) lead to

$$\bar{\xi}_{kj}^2 = \frac{\xi_{js}}{1 + e^{-2\varphi_{1j}}} \int_0^{\xi_{js}} \exp[\tanh\varphi_{0j}(\cosh\xi_j - 1)] d\xi_j \approx \frac{\xi_{js}^2}{1 + e^{-2\varphi_{1j}}} \left[1 + \tanh\varphi_{0j} \left(\frac{\sinh\xi_{0j}}{\xi_{0j}} - 1 \right) \right] \quad (17)$$

where $k = 1$ if $j = w$ and $k = 2$ if $j = o$. Using Eqs. (16) and (17), ξ_{js} and φ_{0j} can be determined from Q and $\bar{\xi}_{kj}^2$. The linearized PBE can only be used when $\Delta\varphi_j < 1$, which implies $\xi_{js} \leq 1.32$ in the case of maximum polarization, $\tanh\varphi_{0j} \approx 1$.

In the micellar case ($m = 2$), the solution of the linearized PBE in phase w is

$$\varphi_w(\xi_w) = \tanh\varphi_{0w} \left(\frac{\sinh\xi_w}{\xi_w} - 1 \right) \approx \tanh\varphi_{0w} \left(1 + \frac{\xi_w^2}{20} \right) \frac{\xi_w}{6} \quad (18)$$

and Eqs. (8) and (9) take the form to

$$\frac{2fQ}{C_{w0}} = \tanh\varphi_{0w} \left(\cosh\xi_{ws} - \frac{\sinh\xi_{ws}}{\xi_{ws}} \right) \approx \tanh\varphi_{0w} \left(1 + \frac{\xi_{ws}^2}{10} \right) \frac{\xi_{ws}}{3} \quad (19)$$

$$\bar{\xi}_{1w}^2 = \frac{3}{\xi_{ws}(1 + e^{-2\varphi_{1w}})} \int_0^{\xi_{ws}} e^{\varphi_w} \xi_w^2 d\xi_w \approx \frac{2\xi_{ws}^2}{(1 + e^{-2\varphi_{1w}})^2} \quad (20)$$

where the last approximation in Eq. (20) is valid when $\xi_{ws} < 1$. Thus, the relation between Q and the potential drop in phase w is $\Delta\varphi_w = \varphi_w(\xi_{ws}) \approx fQ/(C_{w0} + 3fQ/10)$. The condition $\Delta\varphi_w < 1$ implies $\xi_{ws} \leq 2.18$ in the case of maximum polarization of micelles, $\tanh\varphi_{0w} \approx 1$; this upper bound on ξ_{ws} increases with decreasing φ_{0w} . Similarly, the solution of the linearized PBE in phase o is

$$\varphi_o(\xi_o) = \tanh \varphi_{o0} \left(\frac{\xi_{oL} \cosh \xi_o - \sinh \xi_o}{\xi_{oL} - \xi_o} - 1 \right) \quad (21)$$

and Eq. (11) reduces to

$$\frac{2fQ}{C_{o0}} = \tanh \varphi_{o0} \frac{(\xi_{oL}^2 - \xi_{oL}\xi_{os} - 1) \sinh \xi_{os} + \xi_{os} \cosh \xi_{os}}{(\xi_{oL} - \xi_{os})^2} \xi_{os} \quad (22)$$

The potential drop in phase o is $\Delta\varphi_o = \varphi_o(\xi_{os})$ with $\xi_{oL}/\xi_{os} = L/L_o = [1 - (1 - \Phi_o)^{1/3}]^{-1}$. In the regime of maximum polarization, $\tanh \varphi_{oj} \approx 1$, Eqs. (21) and (22) lead to $\Delta\varphi_o \approx (1 + a\xi_{os}^2)\xi_{os}^2(3L - L_o)/6(L - L_o)$ and $2fQ/C_{o0} \approx (1 + b\xi_{os}^2)\xi_{os}^2V_o/A_oL_o$, where $a = (5L - L_o)/20(3L - L_o)$ and $b = (5L^2 - 5LL_o + L_o^2)/10(3L^2 - 3LL_o + L_o^2)$. The relation between Q and the potential drop in phase o is $\Delta\varphi_o \approx fQ/(C'_{o0} + dfQ)$ where $C'_{o0}/C_{o0} \approx (V_o/A_oL_o)3(L - L_o)/(3L - L_o) \approx 1$ and $d = (b - a)6(L - L_o)/(3L - L_o) \approx 1/6$.

Exact solution of the PBE in lamellar microemulsions. It is known since the work of Verwey and Overbeek that the solution of the PBE in planar geometry may involve elliptic integrals [26]. The exact solution of Eqs. (7) and (10) in the lamellar case is

$$\varphi_j(\xi_j) = -2 \ln[\text{cd}(u_j | \alpha_j)] \quad (j = w, o) \quad (23)$$

and Eqs. (8), (9), (11) and (12) take the form

$$fQ/C_{j0} = (1 - \alpha_j)u_{js} \text{sc}(u_{js} | \alpha_j) \text{nd}(u_{js} | \alpha_j) \quad (24)$$

$$\bar{\xi}_{kj}^2 = 2u_{js} \int_0^{u_{js}} \frac{du_j}{\text{cd}^2(u_j | \alpha_j)} \quad (k = 1 \text{ if } j = w, k = 2 \text{ if } j = o) \quad (25)$$

where $u_j \equiv \xi_j/[2(1 + \alpha_j)]^{1/2}$ and $u_{js} \equiv \kappa_j L_j/[2(1 + \alpha_j)]^{1/2}$; $u_w^2 \equiv r^2 F^2 c_{1w}(0)/2\epsilon_o \epsilon_w RT$ and $u_o^2 \equiv (L - r)^2 F^2 c_{2o}(L)/2\epsilon_o \epsilon_o RT$ are independent of $c_{2w}(0)$ and $c_{1o}(L)$, respectively. In Eqs. (23)-(25), $\text{cd}(u|\alpha)$, $\text{sc}(u|\alpha)$ and $\text{nd}(u|\alpha)$ are Jacobi elliptic functions of argument u and parameter α . In the limit $\alpha \rightarrow 0$, they reduce to trigonometric functions, $\text{cd}(u|\alpha) \approx \cos u$, $\text{sc}(u|\alpha) \approx \tan u$ and $\text{nd}(u|\alpha) \approx 1$, and in the limit $\alpha \rightarrow 1$, they reduce to hyperbolic trigonometric functions, $\text{cd}(u|\alpha) \approx 1 - (1/2)(1 - \alpha) \sinh^2 u$, $\text{sc}(u|\alpha) \approx \sinh u$, and $\text{nd}(u|\alpha) \approx \cosh u$. Due to the periodicity of the cd elliptic function, the following restriction applies $u_{js} < K(\alpha_j)$, where $K(\alpha_j)$ is the complete elliptic integral of the first kind. This condition is satisfied if $\xi_{js} < \pi/2^{1/2} \approx 2.22$ because $K(\alpha_j)$ is monotonously increasing function of α_j , with minimum value $K(0) = \pi/2$. However, when $\xi_{js} > \pi/2^{1/2}$ the condition $K(\alpha_j) > u_{js}$ requires that $\alpha_j > \alpha_{j,\min}$ with $u_{js} = K(\alpha_{j,\min})$. Figure 2 shows that the solution of the linearized PBE, Eqs. (15)-(17), may provide a good approximation to the exact solution for lamellar microemulsions; especially in the case of the counterion concentration and the potential drop.

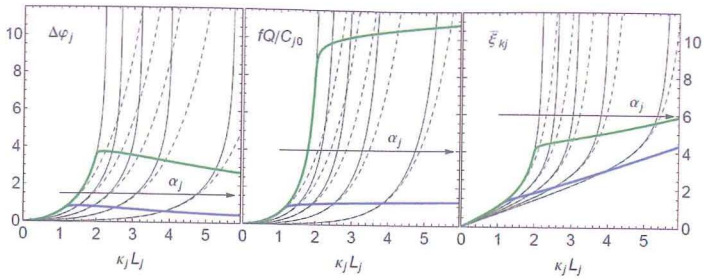


Figure 2. The thick solid lines describe the dimensionless potential drop $\Delta\varphi_j$, charge fQ/C_{j0} and counterion concentration \bar{c}_{kj} in phase j ($j = w, o$) as a function of $\xi_{js} \equiv \kappa_j L_j$ for different values of α_j (0.001, 0.25, 0.50, 0.75, and 0.95 increasing in the arrow direction) in a lamellar microemulsion with $\Phi_s = 0.15$. The lower curve corresponds to the aqueous phase and the upper one to the organic phase. The thin solid lines correspond to the exact solution, Eqs. (23)-(25) and the dashed lines to the solution of the linearized PBE, Eqs. (15)-(17).

The values of c_w and c_o that determine Q_j , \bar{c}_{1w} and \bar{c}_{2o} can be found by iteration imposing Eq. (1), $K_{w/o}c_{2o}(L)/c_{1w}(0) = \alpha_w^{1/2}/\alpha_o^{1/2}$, and Eq. (3). An alternative iteration procedure consists of starting from a value of u_{ws} and expressing u_{os} as a function of α_w and α_o using Eq. (1) as $u_{os} = u_{ws}L_o\varepsilon_w^{1/2}\alpha_w^{1/4}/(L_wK_{w/o}^{1/2}\varepsilon_o^{1/2}\alpha_o^{1/4})$. Then, Eq. (24) for $j = w$ is used as the definition of $Q(\alpha_w) \equiv C_{w0}(1-\alpha_w)u_{ws} \text{sc}(u_{ws}|\alpha_w) \text{nd}(u_{ws}|\alpha_w)/f$, and the distribution potential is written as $z_1 f \Delta_o^w \phi = fQ(\alpha_w)/C_s - 2 \ln[\text{cd}(u_{ws}|\alpha_w) \text{cd}(u_{os}|\alpha_o)]$. Next, α_w and α_o are determined from Eq. (3), $z_1 f \Delta_o^w \phi = z_1 f \Delta_o^w \phi_s + (1/2) \ln(\alpha_w \alpha_o)$, and Eq. (24) for $j = o$, $Q(\alpha_o) = C_{o0}(1-\alpha_o)u_{os} \text{sc}(u_{os}|\alpha_o) \text{nd}(u_{os}|\alpha_o)/f$. Finally, \bar{c}_{1w} and \bar{c}_{2o} are determined from Eq. (25), and c from Eq. (4).

The complexity of this exact solution makes convenient the analysis, in the next subsections, of two limiting cases which provide simple approximate solutions and can also be used to estimate an initial guess of the parameters α_w and α_o to be determined with the routine explained above.

Solution of the PBE in lamellar microemulsions in the regime of maximum polarization. The solution of Eqs. (7) and (10) for lamellar geometry in the regime of maximum polarization ($\tanh \phi_{0j} \approx 1$ and $Q \approx Q_{\text{max}} = FcV_w$) is

$$\varphi_j(\xi_j) = -2 \ln[\cos(\xi_j/2^{1/2})] \quad (j = w, o) \quad (26)$$

where $\xi_{js} < \pi/2^{1/2}$ to avoid the divergence of $\Delta\varphi_j$; the corresponding singularity in \bar{c}_{kj} is associated with the counterion condensation [24]. Equations (8) and (11) reduce to

$$fQ/C_{j0} = (\xi_{js}/2^{1/2}) \tan(\xi_{js}/2^{1/2}) \quad (j = w, o). \quad (27)$$

For low concentrations (i.e. low ξ_{js}), expansion of Eqs. (26) and (27) in powers of ξ_{js}^2 leads to $2\Delta\varphi_j \approx (1 + \xi_{js}^2/12)\xi_{js}^2$ and $2fQ/C_{j0} \approx (1 + \xi_{js}^2/6)\xi_{js}^2$. Hence, the potential drop in phase j can be expressed in terms of the charge as $\Delta\varphi_j \approx fQ/(C_{j0} + fQ/6)$ and the distribution potential is $z_1 f \Delta_o^w \phi \approx fQ[(C_{w0} + fQ/6)^{-1} + C_s^{-1} + (C_{o0} + fQ/6)^{-1}]$. For intermediate concentrations, the values of ξ_{ws} and ξ_{os} must be found from the numerical

solution of Eq. (27). The distribution potential is then evaluated from Eq. (26) as $z_1 f \Delta_0^w \phi = fQ/C_s - 2 \ln[\cos(\xi_{ws}/2^{1/2})\cos(\xi_{os}/2^{1/2})]$; and the values of α_w and α_o from $\alpha_w \alpha_o = \exp[2(z_1 f \Delta_0^w \phi - z_1 f \Delta_0^w \phi_c)]$ and the relation $K_{w/o}(\xi_{os} L_w / \xi_{ws} L_o)^2 \epsilon_o / \epsilon_w = (\alpha_o^{1/2} + \alpha_w^{-1/2}) / (\alpha_w^{1/2} + \alpha_o^{-1/2})$, which follows from Eq. (1) and the definitions of ξ_{js} .

Gouy-Chapman solution of the PBE in lamellar microemulsions. At high concentrations, $\xi_{js} \gg 1$, the electrolyte solutions at $r = 0$ and $r = L$ are approximately electroneutral, $1 - \alpha_j \ll 1$, and the distribution potential reaches the macroscopic value $\Delta_0^w \phi = \Delta_0^w \phi_c$, although Q may still increase with increasing c . The solution of the PBE

$$\varphi_j(\xi_j) = 4 \arctan \left[\tanh(\Delta \varphi_j / 4) e^{\xi_j - \xi_{js}} \right] \quad (28)$$

leads then to the following relation between the potential drop in phase j and the charge

$$fQ/C_{j0} = \xi_{js} \sinh(\Delta \varphi_j / 2). \quad (29)$$

Since $C_{j0} \xi_{js}$ is independent of L_j and proportional to $c^{1/2}$, but Q increases with c more slowly than $c^{1/2}$, it turns out that the potential drop $\Delta \varphi_j$ decreases with increasing c and Q . In other words, the differential capacitances of the aqueous and organic layers are negative. Note that, contrarily to the classical Gouy-Chapman description, Q and $\Delta \varphi_j$ are determined here by the salt concentration and not externally controlled by the electrode polarization. The charge Q is determined from the distribution potential as

$$z_1 f \Delta_0^w \phi_c = fQ/C_s + 2 \operatorname{arcsinh}(fQ/C_{w0} \xi_{ws}) + 2 \operatorname{arcsinh}(fQ/C_{o0} \xi_{os}). \quad (30)$$

The concentrations required to evaluate $\xi_{js} = \kappa_j L_j$ from Eq. (6) can be estimated as $c_{iw}(0) \approx c_{\pm w, \infty} = K_{w/o} c_{\pm o, \infty}$ ($i = 1, 2$) with $c_{io}(L) \approx c_{\pm o, \infty} \approx r_{w/o} [c(c - c_{cr})]^{1/2} / (1 + K_{w/o} r_{w/o})$; note that the mass conservation, Eq. (4), cannot be used in this limit of $\xi_{js} \gg 1$.

RESULTS

The simulations presented below correspond to 300 K, the surfactant Tergitol-10 ($\epsilon_s = 3.0$, $L_s = 2.14$ nm) and the organic solvent α, α, α -trifluorotoluene (TFT, $\epsilon_o = 9.3$). For water, we have used $\epsilon_w = 78$. The two solvents have the same volume fraction, $\Phi_w = \Phi_o$. The PDS is lithium tetrakis(pentafluorophenyl borate ethyl etherate (LiTB, $\Delta_o^w \phi_c^+ = 756.6$ mV, $\Delta_o^w \phi_c^- = 616.7$ mV, $\Delta_o^w \phi_c = 686.7$ mV, and $K_{w/o} = 14.97$). For a surfactant volume fraction $\Phi_s = 0.15$, the thicknesses of the aqueous and organic regions in a cell of a lamellar microemulsion are $L_w = L_o = 6.06$ nm. Figure 3 shows the concentration and electric potential profiles for $c = 10$ mM. Under these conditions, the distribution potential is $\Delta_0^w \phi = 570.0$ mV and the charge separation is almost complete (i.e. $Q/FV = 4.118$ mM is close to $Q_{\max}/FV \equiv c_T = 4.25$ mM). The amount of hydrophobic anion that penetrates the aqueous phase is small but not negligible, $\bar{c}_{2w} = 0.307$ mM, and that of hydrophilic cation in the oil phase is a hundred times smaller, $\bar{c}_{1o} = 3.08$ μ M. Consequently, the deviations from electroneutrality are stronger in

the oil phase, $\alpha_o \equiv c_{1o}(L)/c_{2o}(L) \equiv e^{-2\psi_o} = 0.0023$, than in the aqueous phase, $\alpha_w \equiv c_{2w}(0)/c_{1w}(0) \equiv e^{-2\psi_w} = 0.0515$, although very important in both phases.

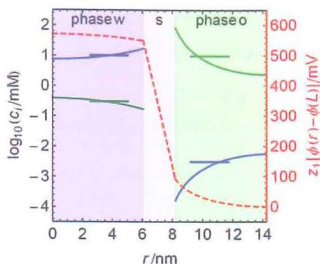


Figure 3. Concentrations of Li^+ and TB^- ions (solid curves) and electric potential (dashed curve) distribution in a globally electroneutral cell of thickness $L = 14.26$ nm a lamellar water[Tergitol-10]/TFT microemulsion with $\Phi_s = 0.15$. The horizontal segments indicate the average ionic concentrations. The microemulsion is formed from $c = 10$ mM LiTB aqueous solution. In order to achieve the distribution equilibrium most TB^- ions transfer to the organic phase, $\bar{c}_{2o} = 9.693$ mM, and very few remain in the aqueous phase, $\bar{c}_{2w} = 0.307$ mM. On the contrary, most Li^+ ions remain in the aqueous phase, $\bar{c}_{1w} = 9.997$ mM, and very few transfer to the organic phase, $\bar{c}_{1o} = 3.08\mu\text{M}$. A distribution potential of 570.0 mV is thus created.

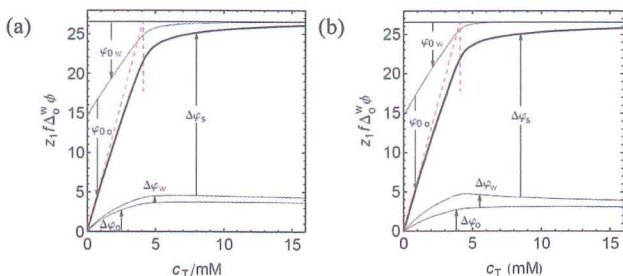


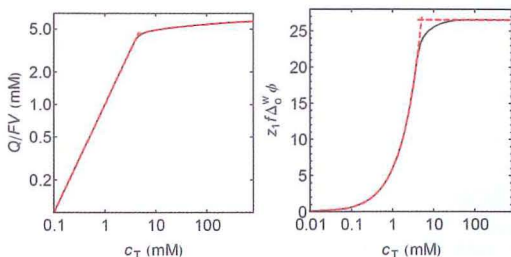
Figure 4. Distribution potential (thick solid line) in a lamellar (a) and micellar microemulsions (b) as a function of the LiTB concentration. The distribution potential is the sum of the potential drops in the three phase (thin solid lines). The potential drop in the surfactant monolayer is the largest, while that in the aqueous phase is the smallest. The dashed lines indicate how the critical concentration is defined. The horizontal line marks the macroscopic distribution potential.

Figure 4 shows the distribution potential in a lamellar microemulsion as a function of the PDS concentration (referred to the total microemulsion volume) for $\Phi_s = 0.15$ and $\Phi_w = \Phi_o$. The interfacial capacitances are $C_{w0}/A \equiv 2\epsilon_0\epsilon_w/L_w = 227.5 \text{ mF/m}^2$, $C_{o0}/A \equiv \epsilon_0\epsilon_o/L_o = 27.12 \text{ mF/m}^2$ and $C_s/A \equiv \epsilon_0\epsilon_s/L_s = 12.39 \text{ mF/m}^2$, so that $C_o = (C_{w0}^{-1} + C_s^{-1} + C_{o0}^{-1})^{-1} = 8.20 \text{ mF/m}^2$. The dashed lines indicate the critical concentration $c_{T,cr} \equiv C_o z_1 \Delta_o^w \phi_o / FV = 4.09 \text{ mM}$ which marks the separation between the regions of almost linear increase of the distribution potential with the total PDS concentration, $c_T < c_{T,cr}$, and saturation towards $\Delta_o^w \phi_o$ when $c_T > c_{T,cr}$. It is remarkable that deviations from local electroneutrality in phase o at $r = L$ persist well above $c_{T,cr}$. The estimated rate of variation of the distribution potential with

the salt concentration (referred to the total volume) is $z_1 \Delta_0^w \phi / c_T \approx FV / C_0 = 168 \text{ mV/mM}$ for $\Phi_s = 0.15$, 113 mV/mM for $\Phi_s = 0.20$ and 67 mV/mM for $\Phi_s = 0.30$.

Figure 5 shows the comparison between the exact solution of the PBE in lamellar microemulsions and its approximate solutions in the regions $c_T < c_{T,cr}$ and $c_T \gg c_{T,cr}$. The distribution potential, separated charge and interfacial capacitance illustrate clearly the two electrical polarization regimes. Because of the gradual decline in microemulsion stability with increasing salt concentration, the theoretical results in Fig. 5, corresponding to very large concentrations, $c \gg c_{cr}$, might not be experimentally relevant but they clearly illustrate the two polarization regimes, which is an important result of the present study. The capacitance changes by less than 40% when the PDS concentration changes by over four orders of magnitude, because it is mainly determined by the surfactant monolayer. At low concentrations, the capacitance is $C_0 = 8.20 \text{ mF/m}^2$ and at large concentrations it tends to $C_s = 12.4 \text{ mF/m}^2$. Hence, the separated charged tends towards $Q_\infty = C_s z_1 \Delta_0^w \phi_s = 6.18 FV$, although reaching this limit would require unrealistically high concentrations. It is noteworthy that the separated charge estimated from the approximations $c_T < c_{T,cr}$ and $c_T > c_{T,cr}$ practically match the exact values. The conclusion is that the solution based on the Jacobi cd elliptic function is only required in a relatively small concentration range corresponding to the transition between the two polarization regimes. It is also remarkable that the solution obtained under the approximation $\alpha_j \ll 1$ when $c_T < c_{T,cr}$, predicts such accurate values of α_j . Observe that $c_{1w}(0) \approx \bar{c}_{1w} \approx c$ and $c_{2o}(L) \approx \bar{c}_{2o} \approx r_{w/o} c$ in the limit $c_T \rightarrow 0$, and hence Eq. (2) imposes that $\lim_{c_T \rightarrow 0} \alpha_w \approx r_{w/o} \exp(-z_1 f \Delta_0^w \phi_s^*)$ and $\lim_{c_T \rightarrow 0} \alpha_o \approx \exp(-z_1 f \Delta_0^w \phi_s^*) / r_{w/o}$.

Figure 6 shows the average and local (at $r = 0$ and $r = L$) ionic concentrations as a function of the total concentration c_T . When $c_T < c_{T,cr}$ the average concentration of minority ions practically vanishes, and when $c_T > c_{T,cr}$ the average concentrations are $\bar{c}_{1w} \approx (c_{cr} + K_{w/o} r_{w/o} c) / (1 + K_{w/o} r_{w/o})$, $\bar{c}_{1o} \approx r_{w/o} (c - c_{cr}) / (1 + K_{w/o} r_{w/o})$, $\bar{c}_{2w} \approx K_{w/o} \bar{c}_{1o}$, and $\bar{c}_{2o} \approx r_{w/o} (c + K_{w/o} r_{w/o} c_{cr}) / (1 + K_{w/o} r_{w/o})$; $Q \equiv F(\bar{c}_{1w} - \bar{c}_{2o}) V_w \approx Q_{cr} \equiv F c_{cr} V_w$ for large c_T .



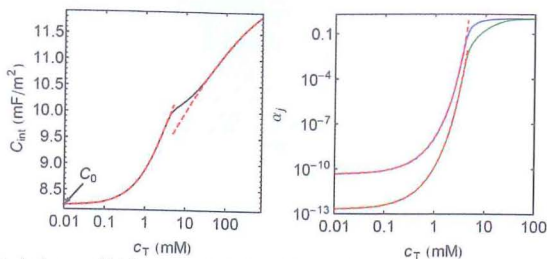


Figure 5. Separated charge, distribution potential and integral capacitance, $C_{int} \equiv Q/\Delta\phi^w$ in a lamellar microemulsion as a function of the LiTB concentration for $\phi_s = 0.15$ and $\phi_w = \phi_o$. The dashed lines are the approximate solutions of maximum polarization (low concentrations) and Gouy-Chapman (high concentrations). The parameters α_w and $\alpha_o (< \alpha_w)$ estimated from the maximum polarization approximation are shown in the last panel.

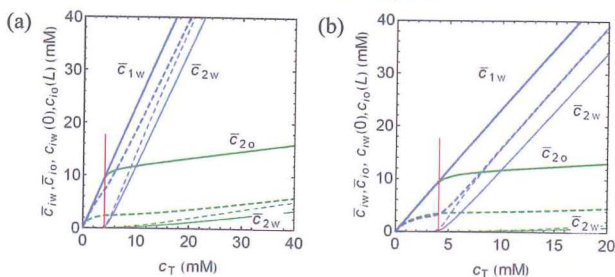


Figure 6. Average (solid lines) and local (at $r = 0$ and $r = L$, dashed lines) ionic concentrations in a lamellar (a) and micellar microemulsions (b) as a function of the LiTB concentration for $\phi_s = 0.15$. The thick lines correspond to the majority species (1 in phase w and 2 in phase o) and the thin ones to the minority species. The (average) concentrations are larger in the aqueous phase (blue lines) than in the organic phase (green lines) because the LiTB water-TFT partition coefficient is $K_{w/o} = 14.97$. The vertical line indicates the critical concentration $c_{T,cr}$.

CONCLUSIONS

The distribution potential in lamellar and water-in-oil microemulsions composed of the aqueous solution of a PDS, an oil and a non-ionic surfactant has been studied and its dependence on the nature and concentration of the PDS, the surfactant concentration, and the geometry of the emulsion microstructure has been explained. The theoretical model used is based on the uniform electrochemical potentials of the ions throughout the microemulsion, the mass conservation, and the global electroneutrality. The charge separation required to build up the distribution potential depends on the characteristics of the microemulsion and, particularly, on its interfacial capacitance. The comparison between the charge available in the microemulsion and the charge required to establish the macroscopic distribution potential $\Delta\phi_o^w$ determines a critical concentration value $c_{T,cr}$ that separates two regimes where the electrical polarization of the microemulsion has different characteristics. The regime $c_T < c_{T,cr}$ cannot be observed in macroscopic ITIES because $c_{T,cr}$ is extremely small for those systems. The different behaviour of electrified microemulsions and macroscopic ITIES is more evident for large surfactant volume fractions. For

low salt concentrations, $c_T < c_{T,cr}$, the solvation energy contribution dominates and the minimization of the microemulsion free energy is achieved by maximizing the charge separation. As confirmed experimentally [8], the phases w and o contain then only counterions, even though this implies a very low microemulsion entropy. The distribution potential and the separated charge increase linearly with c_T in this maximum polarization regime. For high concentrations, $c_T > c_{T,cr}$, the solutions asymptotically approach local electroneutrality at the points furthest from the interface, and the distribution potential saturates to its macroscopic value. The potential drops in the aqueous and organic phases decrease slowly with increasing c_T , while the separated charge increases slowly. Approximate solutions of the PBE equation for these two electrical polarization regimes have been presented. It has been concluded that the exact solution based on Jacobi elliptic functions (in lamellar microemulsions) is only required in a relatively small concentration range corresponding to the transition between the two polarization regimes. Approximate solutions for micellar electrified microemulsions have also been derived and compared to exact numerical results.

Acknowledgements. Financial support from the Ministry of Economy and Competitiveness of Spain (project No. MAT2012-32084) and FEDER, and from the Generalitat Valenciana (project No. GV/PROMETEO2012/0069) is acknowledged.

References

- [1] Sottman, T.; Stubenrauch, C. Phase behaviour, interfacial tension and microstructure of microemulsions, in Stubenrauch C. (Ed.) *Microemulsions*, John Wiley & Sons, Chichester, 2009, chap. 1.
- [2] Lahtinen, R.; Johans, C.; Hakkarainen, S.; Coleman, D.; Kontturi, K. Two-phase electrocatalysis by aqueous colloids, *Electrochem. Commun.* 4, 479-482 (2002).
- [3] Brust, M.; Walker, M.; Bethell, D.; Schiffrin, D.J.; Whyman, R. Synthesis of thiol-derivatized gold nanoparticles in a 2-phase liquid-liquid system, *J. Chem. Soc. Chem. Commun.* 801-802 (1994).
- [4] Liveri, V.T. *Controlled Synthesis of Nanoparticles in Microheterogeneous Systems*, Springer, New York, 2006, chap. 4.
- [5] Peljo, P.; Qiao, L.; Murtomäki, L.; Johans, C.; Girault, H.H.; Kontturi, K. Electrochemically controlled proton-transfer-catalyzed reactions at liquid-liquid interfaces: nucleophilic substitution on ferrocene methanol, *ChemPhysChem* 14, 311-314 (2013).
- [6] Johans, C.; Kontturi, K. Electrochemically driven emulsion inversion, *J. Phys.: Condens. Matter* 19, 375102 (2007).
- [7] Vierros, S.; Iivonen, T.; Johans, C. Measurement of the potential across the oil-water interface in microemulsion, *Electrochem. Commun.* 20, 33-35 (2012).
- [8] Johans, C.; Behrens, M.; Bergquist, K.E.; Olsson, U.; Manzanares, J.A. Potential determining salts in microemulsions: interfacial distribution and effect on the phase behavior, *Langmuir* 20, 15738-46 (2013).
- [9] Shapovalov, V.L. New charged microheterogeneous system- A microemulsion with droplets of variable electrostatic potential, *Russ. Chem. Bull.* 41, 1756-1761 (1992).
- [10] Il'ichev, Yu.V.; Shapovalov, V.L. Effect of the electrostatic potential of microemulsion droplets on photoprotolytic dissociation of 1-naphthol, *Russ. Chem. Bull.* 41, 1762-1767 (1992).
- [11] Roozeman, R.J.; Liljeroth, P.; Johans, C.; Williams, D.E.; Kontturi, K. Dynamic Interfacial Tension at Electrified Liquid/Liquid Interfaces, *Langmuir* 18, 8318-8323 (2002).
- [12] Kakiuchi, T.; Senda, M. Thermodynamics of the electrocapillarity of oil-water interfaces, *Bull. Chem. Soc. Jpn.* 56, 2912-2918 (1983).
- [13] Markin, V.S.; Volkov, A.G. Potentials at the interface between two immiscible electrolyte solutions, *Adv. Colloid Interface Sci.* 31, 111-152 (1990).

- [14] Kakiuchi, T. Equilibrium electric potential between two immiscible electrolyte solutions, in Volkov, A.G. and Deamer, D.W. *Liquid-Liquid Interfaces. Theory and Methods*, CRC, Boca Raton, 1996, chap. 1.
- [15] Manzanares, J.A.; Allen, R.M.; Kontturi, K. Enhanced ion transfer rate due to the presence of zwitterionic phospholipic monolayers at the ITIES, *J. Electroanal. Chem.* 483, 188-196 (2000).
- [16] Murtomäki, L.; Manzanares, J.A.; Mafé, S.; Kontturi, K. Phospholipid at liquid-liquid interfaces and their effect on charge transfer, in Volkov, A.G. *Liquid Interfaces in Chemical, Biological and Pharmaceutical Applications*, Marcel Dekker, New York, 2001, chap. 22.
- [17] Hung, L.Q., Interfacial potential and distribution equilibria between two immiscible electrolyte solutions, in Volkov, A.G. *Interfacial Catalysis*, Marcel Dekker, New York, 2003, chap. 5.
- [18] Kakiuchi, T. Limiting behavior in equilibrium partitioning of ionic components in liquid-liquid two-phase systems, *Anal. Chem.* 68, 3658-3664 (1996).
- [19] Markin, V.S.; Volkov, A.G. Distribution potential in small liquid-liquid systems, *J. Phys. Chem. B* 108, 13807-13812 (2004).
- [20] Volkov, A.G.; Markin, V. S. Electrical properties of oil/water interfaces, in Petsev, D.N. (Ed.), *Emulsions: Structure, Stability and Interactions*, Elsevier, Amsterdam, 2004, chap. 4.
- [21] Aoki, K.; Li, M.; Chen, J.; Nishiumi, T. Spontaneous emulsification at oil-water interface by tetraalkylammonium chloride, *Electrochem. Commun.* 11, 239-241 (2009).
- [22] Samec, Z.; Kakiuchi, T. Effect of the phase volume ratio on the potential of a liquid-membrane ion-selective electrode, *Anal. Chem.* 76, 4150-4155 (2004).
- [23] Kuwabara, S. The forces experienced by randomly distributed parallel circular cylinders or spheres in a viscous flow at small Reynolds numbers, *J. Phys. Soc. Jpn.* 14, 527-532 (1959).
- [24] Tsao, H.-K. Effects of salt addition on the ion distribution enclosed in a cylinder and a sphere. *Langmuir* 15, 4981-4988 (1999).
- [25] Kontturi, K.; Murtomäki, L.; Manzanares, J.A. *Ionic Transport Processes*, Oxford U.P., Oxford 2015, p. 154.
- [26] Verwey, E.J.W.; Overbeek, J.Th.G. *Theory of the Stability of Lyophobic Colloids*, Elsevier, New York-Amsterdam, 1948, chap. 4.

**LA INVESTIGACIÓN DEL GRUPO ESPECIALIZADO DE
TERMODINÁMICA DE LAS REALES SOCIEDADES ESPAÑOLAS DE
FÍSICA Y DE QUÍMICA 2015**